University of Exeter coursework header sheet

Marker, please refer to marking guidelines at http://ex.ac.uk/dyslexia-marking-guidelines

ECMM102 Group Project (Meng) (A, TRM1+2 2016/7)

003771

1027442

Coursework: Individual contribution to the group achievement

Submission Deadline: Thu 4th May 2017 12:00

Personal tutor: Dr Hao Qin

620012789

Marker name: G_Tabor

Word count: 10496

By submitting coursework you declare that you understand and consent to the University policies regarding plagiarism and mitigation (these can be seen online at www.exeter.ac.uk/plagiarism, and www.exeter.ac.uk/mitigation respectively), and that you have read your school's rules for submission of written coursework, for example rules on maximum and minimum number of words. Indicative/first marks are provisional only.

First marker's comments	Indicative mark
Second marker's comments	Second mark
Moderator's comments	Agreed mark

I2 Report

The development of an automatic numerical draft tube model

Patrick Burns

2017

4th year MEng Group Project

I certify that all material in this thesis that is not my own work has been identified and that no material has been included for which a degree has previously been conferred on me.

Signed 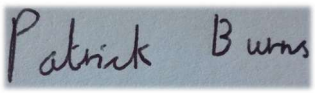 .....

College of Engineering, Mathematics, and Physical Sciences

University of Exeter

I2 Report

ECMM102

Title: The development of an automatic numerical draft tube model

Word count: 10496

Number of pages: 40

Date of submission: Thursday, 04 May 2017

Student Name: Patrick Burns

Programme: MEng Mechanical Engineering with International Study

Student number: 620012789

Candidate number: 003771

Supervisor: Professor Gavin Tabor

Acknowledgement:

I would like to thank Dr Gavin Tabor for his commitment, support and enthusiasm towards the project. I also wish to extend my gratitude to Steven Daniels and Alma Rabat who dedicated enormous time and effort into ensuring the project was a success. Always making time to assist in the project's progression and increase my understanding of OpenFOAM and optimisation techniques.

Most importantly, I'm extremely grateful for the endless support my parents provided throughout my studies at the University of Exeter.

Abstract

Optimisation has become a vital aspect of the design process. The developments in modelling techniques and increases in computational power has allowed for its application to a huge array of design problems. The successful implementation of optimisation to a hydraulic draft tubes design would be hugely advantageous. As minor gains in more efficient energy production translates into huge savings over the operating lifespan of the equipment. Optimisers are able to be indiscriminately applied to systems encoded into a series of objective functions and control variables. The role of Computational Fluid Dynamics (CFD) is to enable the application of optimisation to a real world case.

This report outlines the development of an automatic numerical draft tube model synchronised with Bayesian optimisation. The purpose of the model is to provide function evaluations for the optimisation process. An array of potential draft tube geometries are requested for evaluation and require automatic modelling in order to deliver a corresponding objective function evaluation. The evaluative data calculated needs to accurately represent a draft tube to ensure the near optimum solution translates to an improved real world design. Optimisation demands numerous sample iterations of the evaluative function, therefore the computational efficiency of the model is of vital importance.

The model produced in this study combined fixed and variable meshes reducing the mesh generating process for each sample iteration. The numerical model was able to accurately capture trends between draft tube geometries and the objective function. This was validated by experimental data and enabled its use for optimisation. The results showed the model was limited to a two control point parametrisation, as the structured meshing strategy struggle to produce suitable meshes for geometries containing extreme curvature.

The report also presents a sensitivity study of prescribed draft tube inlet conditions to the pressure recovery factor. The results show significant sensitivity to a range of predicted inlet velocity profiles. However, it was indicated that the ability of the draft tube model to identify designs of desirable pressure recovery factors were unaffected.

Keywords:

Optimisation, OpenFOAM, Hölleforsen Draft Tube, blockMesh, swak4FOAM

Table of contents

1. Introduction and background

1.1. Project Overview

The work documented with in this individual report contributes to a group project aiming to apply machine learning and computational fluid dynamics (CFD) to optimise a draft tube for a low head hydraulic turbine. The group project can be categorised in to three sub groups integrated together to meet the overall project objective. The experimental, CFD and optimisation sub teams have individual, interconnected objectives ensuring the automatic optimisation of a hydraulic draft tube validated through experimental data. Figure 1.1 visually represents the connection between the individual team objectives. This report focuses on the CFD sub team challenge to develop accurate and automatically adjustable numerical models.

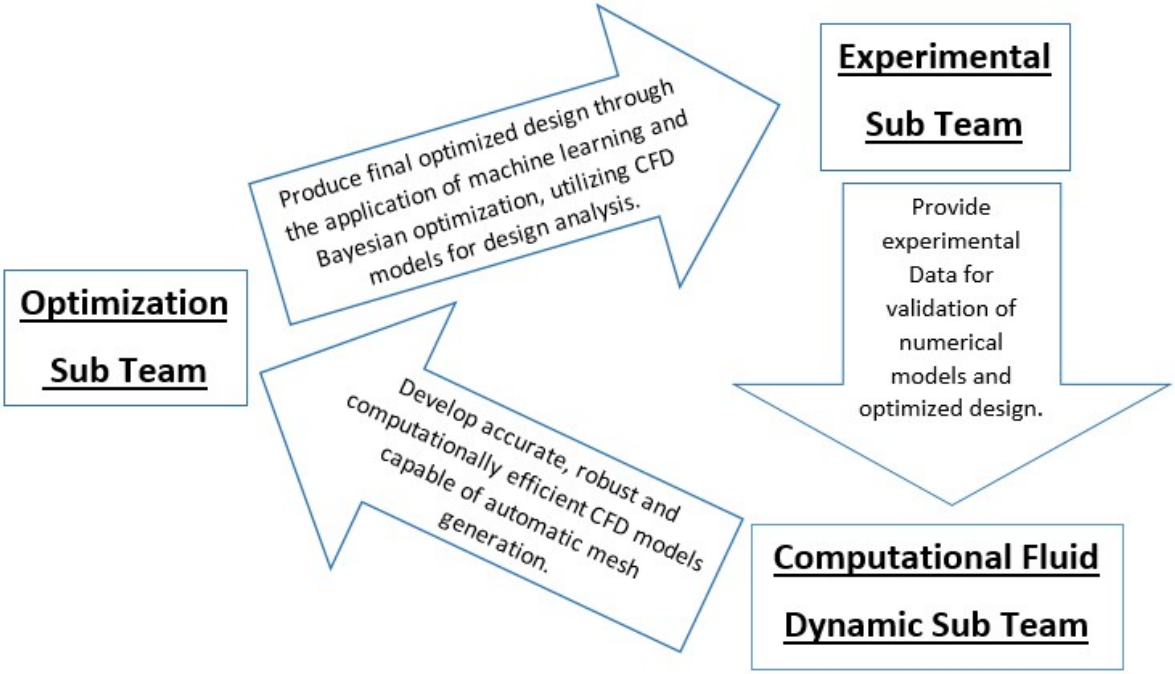

Figure 1.1: Sub team project break down

In order for machine learning based optimisation of a draft tube to be successfully implemented, the CFD sub team are required to deliver a validated numerical model that can be automatically adjusted and integrated with the optimisation code. The purpose of the computational model is to enable systematic analysis of potential design solutions. The design problem is characterised and simplified through an objective function, which can be indiscriminately optimised.

The objective function establishes the quality of the potential solutions and enables

relationships between input parameters to be determined and exploited by the optimisation technique. The corresponding data for the objective function is determined through CFD evaluations. The group project aims to implement Bayesian optimisation, which enables effective function evaluations, resulting in the efficient use of the resource intensive CFD model. This is a novel technique with minimal literature focused on its application with CFD models. The effectiveness of the optimisation technique does not diminish the vital importance of the computational model to provide accurate evaluative data. It aims to reduce the amount of computational data required.

1.2. CFD Team Objective

The purpose of the computational model is to provide the definitive analytical value used to evaluate potential designs. The optimisation is an iterative process that generally requires hundreds of evaluations. There have been extensive efforts within the optimisation community to reduce the number of function evaluations required from resource intensive numerical models, through more effective sampling of data and the establishment of surrogate functions [1]. Despite significant progress the simulation time, especially for complex flow problems, still represents a major hurdle. Therefore, a strong emphasis has to be placed on the model's computational efficiency. However, simplification of models cannot inhibit the model's ability to encapsulate the flow trends governing the design problem.

High fidelity models are essential for the successful application of an optimised design. This gains increased significance with regards to the overall group project, where the optimisation team has placed great emphasis on more effective sampling techniques. The sampling techniques, Bayesian and Adjoint optimisation aim to derive further information from the evaluative data sets provided through CFD, underlining the importance that the primary data set accurately represents the real world case. Draft tubes contain complex flow characteristics that are difficult to numerically represent and require substantial computational effort [2]. This presents a major challenge for the CFD model to establish a suitable trade-off between computational efficiency and model accuracy. Model accuracy is determined through comparisons with experimental results. The experimental team within the project provided results specific to draft tube geometry requested by the CFD team.

The optimiser can request any potential solution within the problem space, which translates

into a CFD model having to automatically generate and simulate a large variety of draft tube geometries. It is essential for successful integration between the optimisation and CFD that a robust model able to accurately provide evaluative data across the entire problem space is developed. The automatic adaptation of the model requires an appropriate meshing strategy and turbulence model to be applied to an array of cases with different flow characteristics. The challenge is to determine universal modelling techniques that allow for stable simulations over a range of geometries, while maintaining the sensitivity to fully define the differences between solutions. The sensitivity to differentiate between solutions is vital in enabling the optimiser to establish relationships between parameters and the objective function.

The aim of the CFD team can be summarised as developing an automatically adjusted draft tube model, identifying a suitable trade-off between the often conflicting characteristics:

- Accurately represent the real world case
- Computationally efficient
- Stability of the solution accuracy to geometric changes

1.3. Individual Objectives

The individual contributions required to ensure the group objectives were delivered was determined within the overall project management of the group. The structure of each individual's objectives and their coordination towards the group's successful optimisation of a draft tube is documented in the overall project report [3]. The individual work packages were integrated together ensuring the group worked effectively to achieve the overall objective. The personal individual objectives detailed in this report are summarised below:

Contribution to the development of the initial SnappyHexMesh automatic model.

The CFD sub team identified the importance of establishing a baseline initial automatic meshing technique using the prominent meshing application SnappyHexMesh. The intention was to focus the sub team's efforts towards an initial technique that could be further developed and explored. This would ensure the minimum requirement of the CFD sub team was satisfied, as well as attempting to mitigate against delays that would affect the optimisation team.

Development of individual automatic meshing technique BlockMeshStitch.

The development of an alternative meshing technique provides options for the optimisation and can be used in comparison of near optimal solutions, enabling diverse validation of the optimised result.

Inlet conditions replicating the experimental setup.

Modelled results are sensitive to the prescribed boundary conditions. Thus, it is vital that the inlet flow conditions replicate the experiment used to validate the numerical models. The representative inlet conditions can then be implanted on all CFD draft tube models.

Determine suitable constraints for the optimisation problem space.

The bounding box constrains potential locations of the draft tube geometry, which hugely influences the level of robustness required from the computational models as well as the range of potential near optimum solutions. The establishment of the appropriate region then permits effective sampling of potential draft tube geometries for experimental results.

1.4. Project Background

The utilisation of hydroelectric power is essential in tackling the challenge of clean energy generation. It is the leading source of renewable energy supplying approximately 20% of the world's electricity and representing about 65% of the electricity generated via renewable energies [2]. The draft tube's main function within a hydraulic turbine is to decelerate the flow in a stable manner. Thus, converting excess kinetic energy into static pressure resulting in a region of low pressure at the draft tube's inlet. The low pressure at the inlet increases the fluid momentum change across the turbine. The coupling of numerical modelling alongside optimisation methods has been exploited by industry in order to minimise energy losses during power generation. The process of integrating optimisation methods with computational modelling has provided near optimal designs implemented within the industry. The literature surrounding the topic consistently highlights the potential of coordinating the two techniques [4].

The draft tube optimisation group project focuses on a single objective function: to maximise the average pressure recovery factor (C_p). This has been identified as the most appropriate objective function from the extensive literature involving the optimisation of a draft tube and

allows for direct comparison with previous studies [5]. The average pressure recovery factor (C_p) is a dimensionless coefficient, where the pressure difference between the outlet and the inlet is normalised by the kinetic energy at the inlet. The group project specified a fixed outlet pressure (P_{out}) set to atmospheric pressure. The flow rate (Q) and the cross-sections at both the inlet (A_{in}) and the outlet (A_{out}) remained constant. The water density (p) was assumed to be constant. Therefore, the objective function can be effectively simplified as minimising inlet Pressure (P_{in}).

$$C_p = \frac{P_{out} - P_{in}}{\frac{1}{2}\rho\left(\frac{Q_{in}}{A_{in}}\right)^2}$$

Equation 1: Average Pressure Recovery Factor.

2. Literature review

2.1. Hölleforsen draft tube model

The computational draft tube models developed in the project were based on the Hölleforsen draft tube model which is extensively documented in the literature [6]. Significantly, the Hölleforsen draft tube has been the subject of multiple papers validating the use of the open source CDF package openFOAM, which was the CFD code used in this project [7], [8]. These studies have confirmed the appropriate use of openFoam to simulate draft tube flow through the successful validation against experimental results and the commercial CFD code CFX. Both papers use the turbulence model K-epsilon with a mesh that yielded a first node wall distance within the range criteria of 2 to 150 with an approximate average of 30. A noticeable abnormality in both papers is the failure for the grid to meet the targeted y plus value of 50. Additionally the specified boundary conditions were based on velocity and pressure measurements detailed in Andersson's, 2000 experiment [6]. At the inlet and the walls a homogeneous Neumann boundary condition was used. The outlet of the draft tube model was set at a constant pressure. The relatively low turbulence levels prescribed at the outlet were regarded of minor importance to the overall flow.

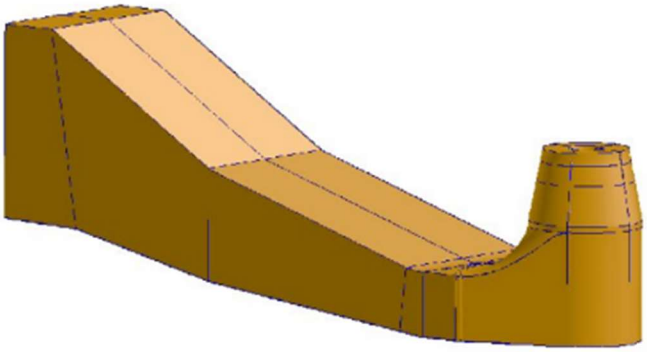

Figure 2.1: Hölleforsen draft tube.

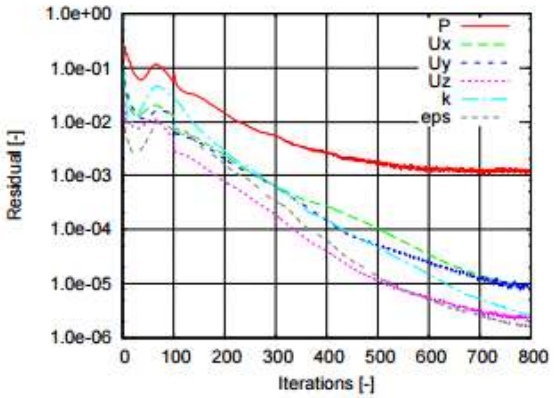

Figure 2.2: Failure of residual to converge.

The openFOAM validation studies emphasise a key feature of steady state draft tube simulations. The residual error fails to fall below $1x10^{-3}$, often considered the point of loose convergence. Figure 2.2 shows the development of the residuals for the draft tube's computation. The residuals drop rapidly in the initial phase of the computation. The residuals develop by oscillating around a mean level which could be acceptable for a complicated case [7]. The unsteadiness in the residuals is inherited from steady state simulation of unsteady flow. This issue was further explored in a 2011 study, which again used openFOAM to simulate the Hölleforsen draft tube [9]. The conclusion drawn from this study was comparison of draft tubes can be achieved with the assumption of steady state flow. This conclusion is significant to our project as it vindicates the use of steady state computations, directly stating it has the predictive capacity to accurately obtain the pressure recovery factor, which is the subject of the project's optimisation function. The consequences of this is a huge reduction in simulation time.

A series of academic workshops between 1999 and 2005 dedicated intense research to the development of an accurate model able to represent complex fluid flow within the Hölleforsen draft tube [10]. The challenge of interpretation of inlet parameters was repeatedly concluded to be a primary cause of deviations between the experimental data and the simulated results. The studies that analysed the results from a number of draft tube models originating from a range of different independent institutions reported a large level deviation between prescribed inlet conditions. The simulated results proved to be sensitive to the inlet condition emphasising the importance of correct representation. The issue of inlet flow representation and parameterisation is a continuing theme as the literature progresses. A 2015 study that optimised hydraulic draft tube components commented on the lack of suitable inlet condition

parameterisation, which inspired the solution of coupling the optimisation of the turbine runner and draft tube [11]. These findings are significant to the project as, although the optimising test case will not have swirling inlet flow, they highlight the sensitivity of the results to the conditions set at the highly turbulent inlet.

2.2. General themes from combined CFD and optimisation

The defining theme that embodies the literature surrounding the integration of CFD and optimisation is to improve the processes computation efficiency and accuracy to experimental data. This provides the motivation for a significant area of research dedicated to developing supplementary techniques which enables the optimisation code to more efficiently diagnose potential designs. Recent studies have demonstrated the potential of surrogate [1] and hierarchical-metamodel-assisted evolutionary algorithm [4] in reducing the dependency of optimisation on large amounts of computationally intensive simulated results. The potential improvements of sampling efficiencies has implications on the priorities of the CFD models between accuracy and computational efficiency. Sampling of simulation results can therefore be less frequent allowing a shift in priority towards model accuracy, rather than running speed.

Repeated optimisation has demanded the simplification of models. This inevitably results in a lower modelling accuracy. However reduced model accuracy is of less significance because of general agreement within the literature regarding the optimisation of a draft tube. The literature asserts capturing global trends is a higher priority than predicting all flow features accurately [1]. Previous work has successfully optimised draft tube design using models unable to represent the full extent of efficiency improvements. One paper optimising a draft tube recorded an optimisation improvement based on CFD results of just 0.02% pressure recovery, however experimental results later proved a pressure recovery gain of 0.5%. It is important to note these small improvements in pressure recovery are subject to multi-objective optimisation, where civil costs were also minimised [12]. These findings provide context to the imperative challenges of developing a robust model capable of obtaining results across a large problem spaces, while ensure to result produce accurately converge to the real life case.

The literature acknowledges the conflict between the need for optimisation efficiency and accuracy of results. Although there are revelations in capacity of optimisation techniques to optimise design problems from models capable of only capturing the general flow, a major trend in the research is the stated need for advancements in CFD model accuracy. Several

influential papers over a significant period of time have consistently stated the need for improved model accuracy. Developments in the appropriate coupling of mesh with turbulence models and the sensitivity of grid refinement have been identified as future work [10]. A recent study in 2014 stated the need for a more sophisticated CFD model integrated into optimisation in order for greater understanding of the effects of more complex flow phenomena [4]. This indicates that more advance optimisation techniques are starting to demand higher model accuracy in the search for an improved near optimum solution.

Model computational efficiency is vital for the progression of combined optimisation and CFD. Over the last decade the emphasis has shifted away from the optimisation of peak efficiently towards the desire to improve weight average efficiency across a range of operating conditions. From 1990 to 2000 peak efficiency of hydraulic turbines was increased only by 0.2%, in spite of extensive application of computer aided design and CFD tools. This suggests that the limit has been nearly reached and any sufficient increase in peak efficiency in future turbine designs is doubtful [13]. Therefore the scope of the optimisation problem has increased to encapsulate a range of operating conditions. This need to optimise over a range of operating conditions has been consistently determined throughout the literature and was reinforced by the feedback from a project visit to Mary Tavy hydro power plant [14]. The need for computational efficiency improvements is further intensified when considering the success of recent papers where the coupling of optimising hydraulic parts prove more advantageous than integrating a series of individually optimised parts. The optimised runner–draft tube geometry outperforms the result of a single runner optimisation by about 0.3% in terms of average efficiency [11].

2.3. Previous Optimised Draft Tubes.

Draft tube optimisation is a topic popular topic within the optimisation community. It has obvious real world benefits to the energy industry, where small gains in efficiency correspond to significant energy savings over the life time of the equipment [15]. Results have shown trends in the near optimum design solutions for draft tubes. The introduction of gradual curvature and a growing increase of the cross sectional area towards the draft tube outlet as exhibited in figures 2.3. Importantly the efficiency improvements quoted in these studies relate to hydraulic efficiency of a turbine defined by equation 2.

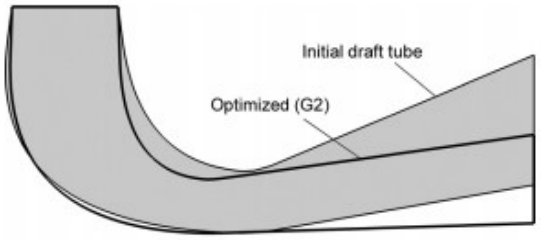

Figure2.3: Resulting draft tube with an efficiency improvement of 1.4%. **[11]**

$$\eta_h = \frac{M\omega}{\rho g Q H} = \frac{H_R}{H}$$

Equation 2: Hydraulic Efficiency of a turbine. H = turbine head, H_R = runner head.

Optimised results targeting pressure recovery factor (C_p) and therefore directly compatible to this study, show improvements in the objective function of around 10%. Figure 2.4 illustrated a draft tube parameterised through interconnecting cross-section, which achieved a pressure recovery improvement of 10.1% [16]. A study that implemented surrogate model based optimisation on the Hölleforsen draft tube outlet diffuser achieved a pressure recovery improvement of 14.4 % and 8.9% for two different flow conditions [1].

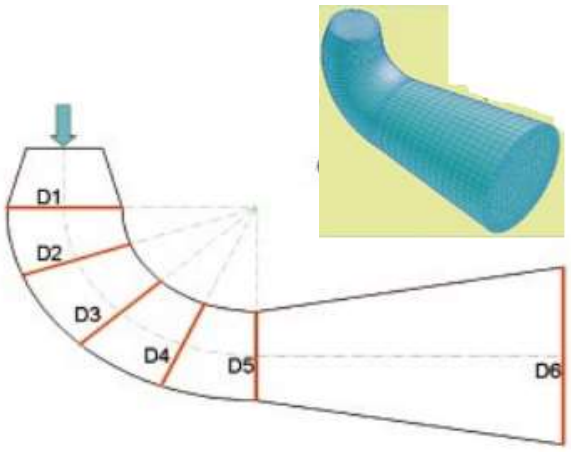

Figure 2.4: Draft tube parameterisation used in the automatic shape optimisation study achieving a pressure recovery improvement of 10.1%. **[15]**

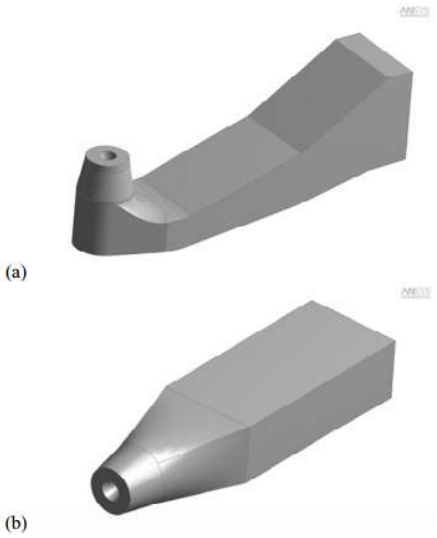

Figure 2.5: Hölleforsen draft tube outlet diffuser surrogate model. **[1]**

2.4. Integration of CFD and Optimisation

The most significant process to integrate CFD and optimisation is the parameterisation of the design problem which encodes the real world situation for optimisation. The choice of shape parameterisation technique has an enormous impact on the formulation of the optimised solution [17]. Parameterisation determines the nature of the adaptations in geometry. The computational cost of an optimisation problem is highly influenced by the number of design

variables. It is advantageous to find a minimum amount of relevant design variables, while not impeding the range of potential solutions possible. Two parametric strategies, Adapted Design and Profile Design, categorises the methods of parametrisation of draft tube geometry in a shape optimisation problem [1]. The adapted design approach replicates traditional CAD dimensions and is often chosen for optimisation featuring the minimisation of civil cost, as they correlate [13]. The profile design approach uses a number of profiles (cross-sections) with different shape, location and orientation along a stacking curve to represent the draft tube geometry. [18]

The two parametrisation approaches have been used consistently within the literature with neither seeming to assert a dominance. Figure 2.6 and 2.7 show the use of each method in recent draft tube optimisation studies.

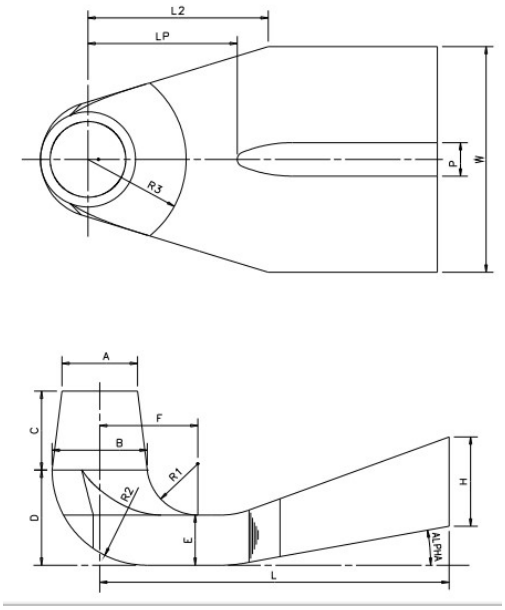

Figure 2.6: Adaptive approach to parametrisation used in a 2015 study. **[11]**

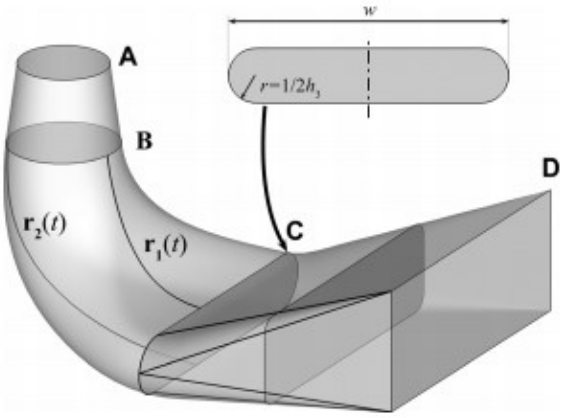

Figure 2.7: Model approach to parametrisation used in a 2014 study. **[4]**

These methods of parametrisation are heavily used for their tendency to produce design that can be practically implemented. The group project proposes the use of Catmull-Clark splines to parametrise the geometry. This technique documented in Hutchings individual report is a less constraining and more abstract method of parametrisation [19]. This novel method of parameterisation enables investigation in the potential of non-uniform draft tube geometries. There are significant repercussions to the robustness required from the computational models as a result of the Catmull-Clark spline method of parameterisation. The abnormal geometries

of the potential design solutions evaluated by the CFD models pose a sizable challenge to maintain mesh quality within the automatic process.

The Daniels and Rahat work on Bayesian optimisation with CFD function analysis heavily influences the group project [20]. There work provides a template to the implementation of Catmull-Clark splines parameterisation. Significantly the importance of maintaining the consistency of the shape and grid quality between sample iterations, while providing flexibility for a wide range of shapes using the same parameterisation of the geometry is emphasised [20]. Their literature suggest a range of possible meshing techniques.

The first is the use of snappyHexMesh which was successfully implemented and therefore will be the first technique explored within this report. A grid distortion method and an immersed boundary method were also reviewed in the literature. The grid distortion process maintains a constant mesh where the cells are distorted in order to match the desire geometry. The potential of the Catmull-Clark spline parameterisation method to produce irregular shapes could cause the distorted mesh to exhibit poor mesh quality. The quoted solution for poor mesh quality experienced by the grid distortion method is increased mesh refinement. The immerse boundary method requires an initial mesh covering the entire potential geometry. Cells not in the desire geometry are blocked out and flow is simulated through the remaining cells. Significantly, this method requires fine grid resolution in order to accurately capture the geometry [20].

3. Development of the Snappy Hex Mesh Model

3.1. Background to snappyHexMesh model

The OpenFOAM snappyHexMesh application is a computer generated mesh sculptor used to produce meshes of complex geometries from a basic initial mesh. SnappyHexMesh required a base hexahedral block mesh and an STL file of the draft tube geometry. The sculpting of the mesh consists of the refinement of elements at the geometry boundary. The refined boundary of the geometry shows a gradual blending of the unstructured mesh aspects, while the core has a structured base mesh. To achieve this snappyHexMesh operates a three stage meshing process involving castellation, snapping and boundary layer refinement. The castellation process identifies cells, which intercept the STL outline and apply a refinement by repeated cell splitting in an attempt to improve matching cell resolution to the geometry. After this

refinement process, all cells which lie “outside” the desired geometric domain are deleted from the mesh. The snapping process snaps vertices on the edge of the domain to the STL surface, using an iterative process of mesh movement, cell refinement and face merging. In the final boundary layer refinement operation, the mesh is moved away from the geometrical surface. Cell layers which are parallel to the geometries outline, are installed. The whole process is robust and automated, but is controlled by a large number of user specified parameters defined in the snappyHexMeshDict document [21].

There are 35 parameter controls within the snappyHexMeshDict that are categorised by refinement controls (10 parameters), snap controls (5 parameters), Layer controls (16 parameters) and mesh quality controls (14 parameters). A study applying genetic algorithm optimisation to improve the quality of meshes produced by snappyHexMesh, reduced the excessive number of parameters by identifying 7 of heightened significance [22]. The work in this report focused on these identified control parameters as well as the “n Cell Between Levels” and “Feature Edge Refinement” parameters in order to identify an appropriate combination that could produce a suitable mesh.

Table 1: Investigated snappyHexMesh parameter.

Snappy Control	Description:
n Cells Between Levels	Defines number of cells for each refinement level. The higher it is, the more gradual the mesh.
Feature Edge Refinement	Specific refinement level for geometry's feature edges
Resolve Feature Angel	Applies maximum level of refinement to cells where an intersections angel above the angle specified.
n Smooth Patches	Alter the number of snapping iterations to the boundary.
n Relax Iterations	Sets number of relaxing script executions that removes poor quality mesh point.
n Feature Snap Iterations	Controls the number of morph iterations within main snapping iterative process.
Max non-Orthogonality	Set the maximum thresholds of acceptable Orthogonality caused by the snap and add on layers processes.
Max Boundary Skewness	Set the maximum thresholds of acceptable skewness caused by the snap and add on layers processes.

SnappyHexMesh was the automatic meshing method used in the Daniels and Rahat study applying Bayesian optimisation to the Pitz Daily OpenFOAM tutorial case [20]. Their study provided the platform for the optimisation model developed within this project, justifying the attempted application of the snappyHexMesh model within the optimisation procedure. The integration between the optimisation and the computational snappyHexMesh model is visually outlined in figure 3.1.

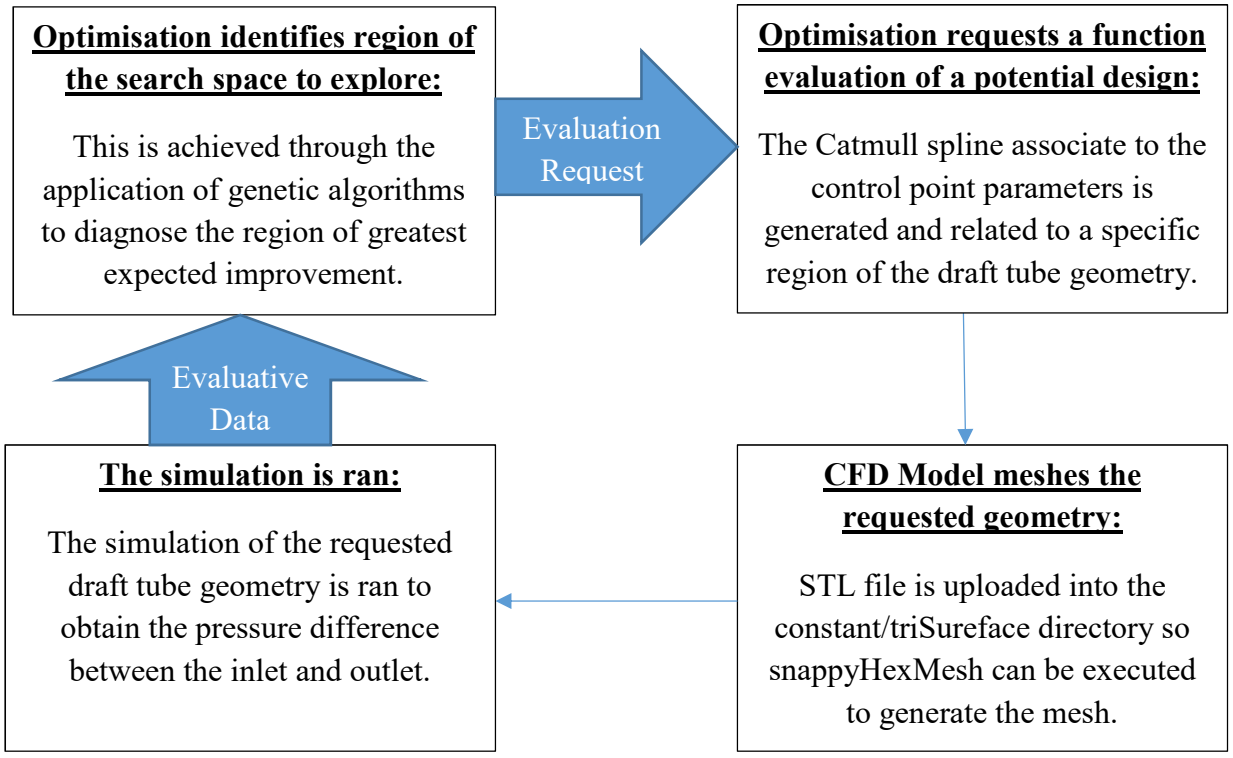

Figure 3.1: Flow chart representing the interaction between the optimisation code and the snappyHexMesh model.

3.2. Mesh requirements

This report focuses on the use of the turbulence model K-epsilon n. The effects of applying alternative turbulence models were investigated in Hardy's individual report [23]. A turbulence model allows for the chaotic nature of the turbulent flow to be encapsulated by a model without applying an unattainable mesh refinement. Turbulence model K-epsilon introduces the use of two new parameters and corresponding new transport equations, turbulent kinetic energy (k) and turbulence dissipation rate (ε). To accurately encapsulate boundary layer flow, a wall function is applied, which requires a prescribed first node wall distance to be satisfied. Previous literature surrounding the draft tube case process determines the use of turbulence model K-epsilon. Therefore, a mesh that yields a first node wall distance within the range criteria of 2 to 150 with an approximate average of 30 is required [7]. The characteristic of the flow case and

the corresponding mesh criteria is displayed in tables 2 and 3. The methods of calculation are shown by equations 3 to 7. The experimental team specified an achievable flow rate of 0.5 litres per second.

$$\Delta y = \frac{y^+ \nu}{u_T}$$

Equation 3: First node wall distance **[22]**

$$u_T = \sqrt{\frac{T_w}{\rho}}$$

Equation 4: Friction Velocity **[31]**

$$T_w = \frac{1}{2} C_f \rho u^2$$

Equation 5: Wall Shear Stress **[22]**

$$C_f = 0.079 Re^{-0.25}$$

Equation 6: Schlichting Skin-Friction Correlation **[22]**

$$\delta = \frac{0.37\, x}{Re^{0.2}}$$

Equation 7: Blasius Boundary Layer Equation for a Flat Plate **[22]**

Table 3:

Draft Tube Characteristics	
Kinematic Viscosity (m^2/s)	1.3070E-06
Flow Rate (m^3/s)	0.005
Inlet Diameter (m)	0.023646
Inlet Velocity (m/s)	1.1386
Estimated Pipe Length (m)	0.17610
Desired Y^+ value	50

Table 2:

Calculated Problem Characteristics:	
Reynolds number	20599
Schlichting skin-friction correlation (C_f)	6.5942E-03
Wall shear stress (T_W)	4.2730
Friction Velocity (U_T)	0.065378
First Node Wall Distance (m)	9.9957E-04
Boundary Layer Thickness (m)	8.9370E-03
Number of Cells in the Boundary Layer	8.9408

A suitable quality of mesh, consistently produced across the entire range of the potential solutions, is required to ensure the accurate evaluation of designs. Localised regions of poor mesh quality can result in drastic repercussions on the model's stability as just one awkward face is sometimes sufficient to destroy convergence [22]. The susceptibility of an automatic

meshing technique to yield catastrophic localised mesh quality, can be monitored through the maximum value of orthogonality and skewness. The OpenFOAM library includes a utility checkMesh which can be run to provide values for average and maximum skewness as well as average and maximum orthogonality. These mesh quality measurements are regularly monitored in the literature. When establishing a mesh quality, the previously mentioned study which implemented genetic algorithms on snappyHexMesh focused on maximum orthogonality and maximum skewness. Skewness and orthogonality were the key indicators used in this report.

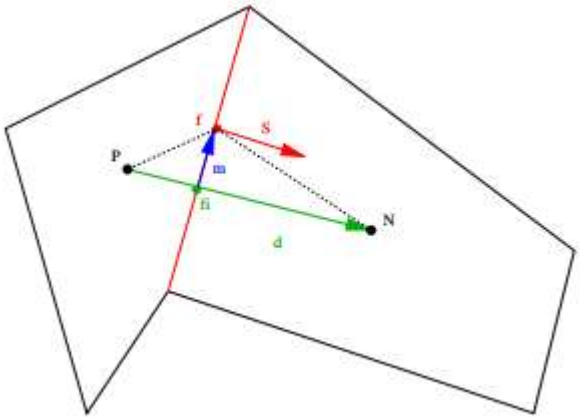

Figure 3.2: Vector use to define mesh quality within OpenFOAM. **[20]**.

Skewness arises from discrepancies between the location of the face centre and the location of the cell centre vector. This is represented in figure 3.2 as the disparity between vector m and vector d. Non-orthogonality arises from misalignment between face normal vectors and the vector connecting adjacent cell centres [24].

The global mesh quality influences the simulator's ability to converge towards the true solution. Poor overall mesh quality is a leading cause for deviations from the real world case [25]. Averaged mesh quality indicators are challenging to interpret and can often be misleading. A more effective classification of global mesh quality is to qualitatively evaluate the mesh using the visualisation software ParaView. Judgements can be based on; the consistency of the shape and size of mesh elements, alignment of elements towards general flow direction and integration of similarly shaped elements.

3.3. Analytical Investigation of the snappyHexMesh method

The experimental results determined within the project were obtained from a 1:20 scaled model of the experimental model used in the draft tube 99 work shop **[5]**, which itself was a 1:11 scaled model of the Hölleforsen draft tube. Angus's individual report documents detailed engineering drawings of the experimental model which was directly simulated by the CFD models **[26]**.

SnappyHexMesh requires an initial basic mesh to be converted into a mesh representative of the desired geometry. The OpenFOAM utility blockMesh was employed to generate a hexahedral structured initial mesh. This initial mesh extended over the entire draft tube STL. The inlet and outlet of the draft tube bordered the initial mesh, which enabled them to be registered as patches where boundary conditions can be applied. SnappyHexMex applied a surface refinement to increase cell resolution at the external geometry of the STL. The coupling of a suitable initial element size and refinement level has to satisfy the required first node wall distance of 0.996mm. The nature of the refinement results in an exponential reduction in the first node wall distance, demonstrated in figure 3.3. The calculated coupling of initial mesh density and surface refinement are stated in Table 4.

Table 4: BlockMesh cell divisions for each refinement level setting in snappy.

	Prescribe blockMesh Structure		
	Number of Cells in the X Dimension	Number of Cells in the Y Dimension	Number of Cells in the Z Dimension
Refinement Level 1	80	50	38
Refinement Level 2	40	25	19
Refinement Level 3	20	13	10

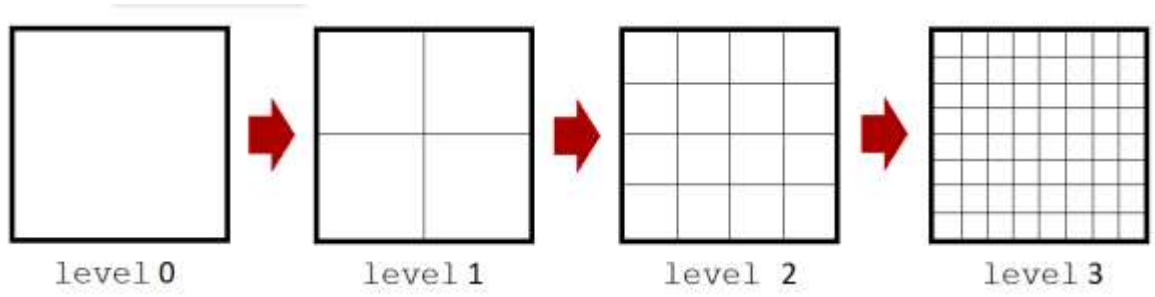

Figure 3.3: Diagram of the refinement level use in OpenFoam.

SnappyHexMesh recommends default settings of the control parameters. A sensitivity study was performed on the highlighted parameters from previous studies to establish their corresponding effects. A lower and upper bound limit away from the default, was determined and meshes for each parameter change were generated. The sensitivity study would give an insight into improved meshing parameters combination. Within the sensitivity study meshing time, average surface displacement and global mesh quality were monitored. For each iteration of the optimisation, a potential draft tube geometry shall be meshed. The meshing time for each integration has a significant implication on the overall running time of the optimisation code.

The surface displacement relates the closeness of the produced mesh to the desired geometry. It records the distance between the external nodes of the mesh to the STL file required by snappyHexMesh, therefore evaluating the ability of the snappyHexMesh settings to impose suitable meshing around areas of complex geometry. The surface displacement was obtained through the offSetMesh external add in, developed in the Fabritius and Tabor 2015 study [22].

Global mesh quality was quantitatively evaluated through a specific mesh quality parameter, developed in partnership with Steven Daniels. The purpose of this mesh quality parameter was to reduce dependency on often subjective, visual inspection. The parameter is a normalised combination of skewness and non-orthogonality. The normalised values were restricted to a fixed range that could be divided and categorised in bands from 0 to 9 indicating the level of mesh quality. A developed utility checkMeshModify stated the percentage of cells within a classified band. Ideally 100% of the cells would demonstrate high mesh quality and be attributed to the lowest band, resulting in a global mesh quality value of 0. Alternatively, extremely poor mesh quality would be where all cells fell into the top band and the global mesh quality would be 9.

This global mesh quality parameter was developed with the additional motivation to penalise poor quality sample models that would omit inaccurate results. However, this was not achieved in this project.

3.4. Analysis of snappyHexMesh

The meshing time for the various meshing settings remained relatively constant at 286s when executed on a computer with 4 cores and 16 gigabyte of ram. This large meshing time poses a major issue for the integration of a snappyHexMesh model. The previous study utilised snappyHexMesh as the automatic meshing technique focused on a two dimensional case [20]. The discovery of the inappropriately large mesh time for the snappyHexMesh meshing technique, delegitimises its use in an optimisation process for a three dimensional case.

The tornado graphs in figure 3.4 and 3.5 present the results of the sensitivity study. The sensitivity of the average surface displacement to the snappy control settings is significantly larger than the global mesh quality. This disparity is due to the consistent hexahedral elements at the core of the mesh biasing the mesh quality metric. The core mesh is relatively unaffected by the snappyHexMesh parameters. Only the "n Cells Between Levels" parameter has a major effect as it increases the influence of the refinement at the mesh core. The average surface displacement analyses the outer refinement layer at the boundary of the mesh. This region is most effected by the snappy refinement, therefore explaining the heightened sensitivity to the quality metric.

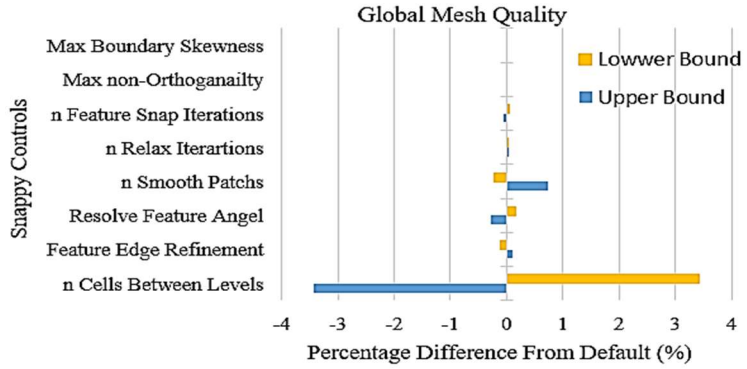

Figure3.4: Tornado graph indicating the sensitivity of global mesh quality to snappyHexMesh control parameters.

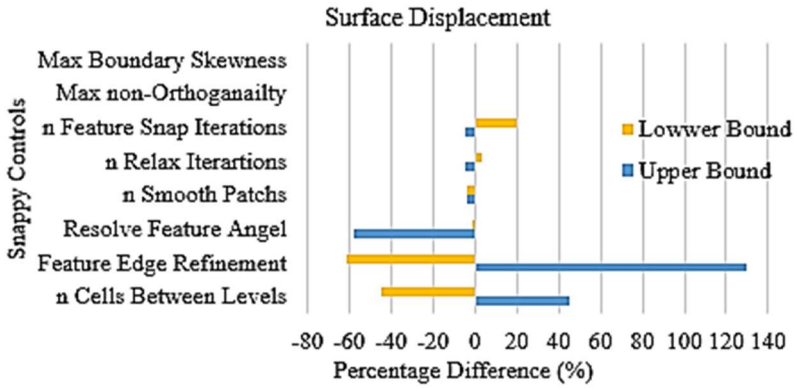

Figure 3.5: Tornado graph indicating the sensitivity of surface displacement to snappyHexMesh control parameters.

Using the sensitivity study as a reference, improved snappyHexMesh parameter settings were interpreted with the objective of minimising both surface displacement and mesh quality. The established improved settings resulted in a significant improvement in maximum surface displacement and a higher quality global mesh, as shown in table 5.

Table 5: Improved snappy settings.

	Default Settings Model	Improved Settings Model
Global Mesh Quality	0.72057	0.69956
Maximum Surface Displacement	0.00158	5.82E-05
Meshing Time (s)	286.04	288.51

Despite the mesh improvements, resulting simulations were unstable and failed within 5000 iterations. Additionally, the indicated average non dimensional wall unit (y^+) value was 17.65, below the targeted 30 required for the k-epsilon turbulence model. The low y^+ values have ramifications on future developments of the snappyHexMesh model. Improvements in mesh quality at the boundary, requires greater refinement to compensate for the uneven snapping process. The constraining first node wall distance intensified the challenge to achieve acceptable mesh quality at the boundary. The addition of cell layering parallel to the mesh boundary, was further investigated and documented in Hardy's individual report [23]. Localised poor mesh quality of the improved snappyHexMesh model can be seen in Figure 3.6. The concaved cells on the edges of the draft tube geometry are the most probable cause for the unstable simulation of flow. The intersected cells at the boundary of the geometry highlight the need for the addition of cell layering parallel to the boundary.

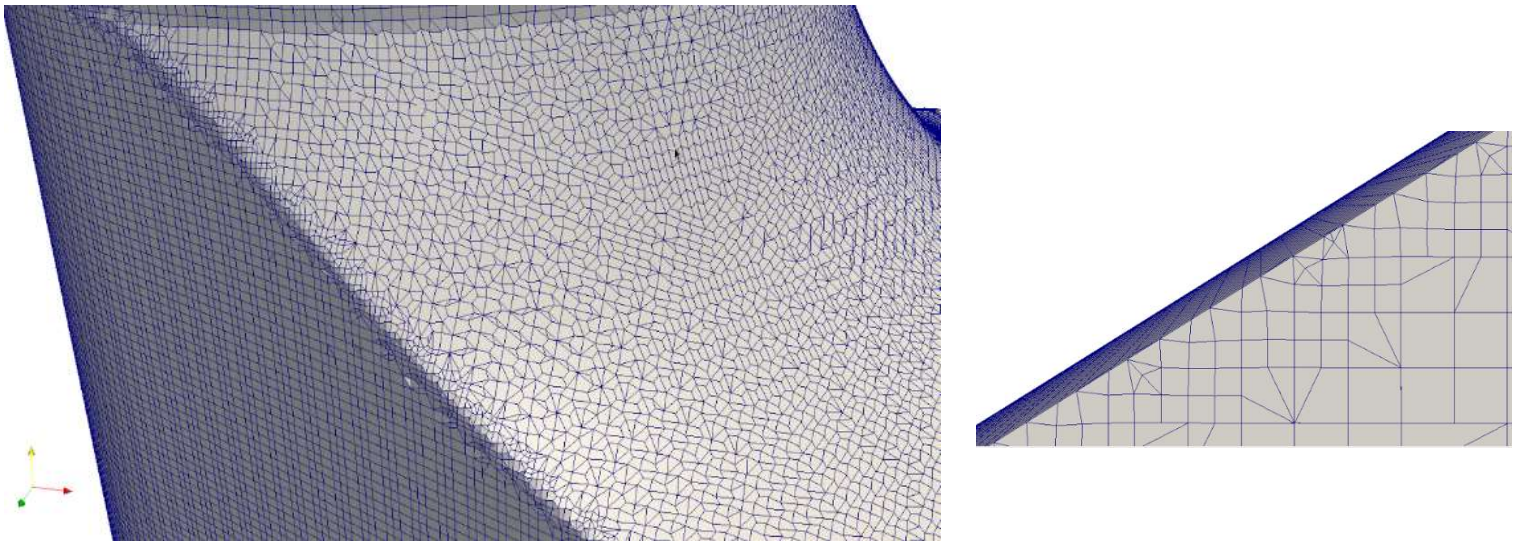

Figure 3.6: Poor mesh quality exhibited by snappyHexMesh. Concaved cells at the edges (left), segmented cells at the boundary (right)

After communication within the group, it was decided that the investigation into alternate meshing techniques would be more advantageous than the continued development of the snappyHexMesh model. This conclusion was drawn due to the excessive meshing time and catastrophic localised mesh quality unable to be alleviated through the traditional approach of increased refinement at the boundary. The clash of the relatively small draft tube model geometry with a relatively large first node wall distance required by the turbulence model has redefined the development of an appropriate automatic meshing technique. The primary focus therefore, has shifted towards introducing the demanded y^+ value, while mesh quality and a suitable grid resolution is maintained. This discovery indicates that the grid distortion and the immersed boundary methods reviewed in the literature, may not be adaptable to this specific problem as they traditionally require increased grid refinement [20].

4. BlockMeshStitch

BlockMeshStitch is an alternative, automatically-altered, computer generated model. It combines an unchanged mesh at the cone and elbow of the draft tube developed, in Pointwise as part of Gowan's individual project [27] and a variable outlet diffuser established within blockMesh. The combination of Pointwise and blockMesh provides a complementary structured meshing approach as part of the design strategy defined in the group project report. [3]

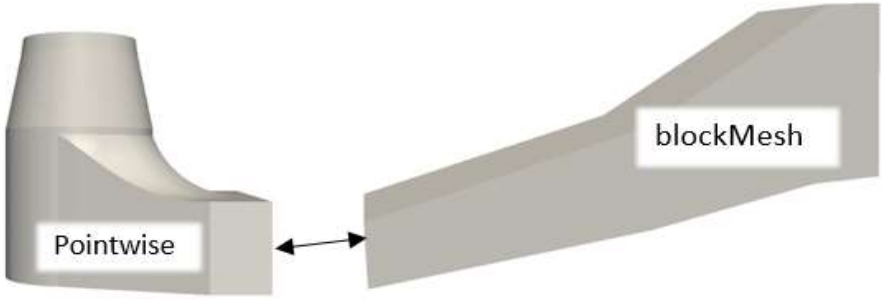

Figure 4.1: BlockMeshStitch Diagram.

4.1. Background to Stitch Mesh Applications

A 2011 paper implemented robust optimisation of a 2D air conditioning duct using an automatic CFD model, which demonstrated the successful integration of a constant and variable mesh within an optimisation project. This technique identified the geometry required to be re-mesh by isolating the region of geometric variability and integrating it with the pre-

existing mesh region for each optimisation sample. The study identified that stitching meshes produced regions of mesh integration that were susceptible to poor mesh quality. The highly skewed region of cells caused the solutions simulated to diverge from the real world case resulting in the identification of a false optimum. These challenges were resolved by ensuring that the mesh profiles between the stitched patches were consistent and that an alternative parameterisation accommodated the fixed geometries [28].

4.2. Design of BlockMeshStitch model

The first stage of the design process was to identify the region of geometric variability. A group decision was made to initially focus on the simplest possible case. Therefore, the lower polyline of the outlet diffuser was diagnosed as the most appropriate region to initially optimise. The boundaries of segmentation between the fixed and variable geometries were determined by the experimental sub team to enable a modular experimental set up. The modularisation of the experiment reduced manufacturing cost, as a major component of the draft tube will remain constant. Therefore, a greater number of potential draft tube designs could be experimentally analysed within the available budget, increasing the amount of experimental data available to validate the models [26].

The generation of the irregular cone and elbow of the Hölleforsen draft tube through the mesh generating software Pointwise is documented in Gowan's individual report [27]. This Pointwise mesh was maintained throughout the optimisation process. An altered diffuser mesh was stitched to the elbow outlet. The uniform nature of the outlet diffuser permitted mesh generation through the OpenFOAM meshing tool blockMesh. A multi block blockMesh topology was used to maintain the unchanged regions either side of the variable geometry. The Bspline utensil to define edge type connecting specified vertices, was utilised to impose the optimiser requested Catmull-Clark spline to the diffuser's mesh. The spline requested for evaluation could then be transferred to the computational model as a csv file. The intersecting points defining the spline in the csv file were at significantly small intervals. Therefore, variation between spline generations techniques were negligible. This was confirmed by the computational engineer who programed the blockMesh Bspline utensil. Consequently, direct

comparisons of other automatic meshing techniques were possible as the Catmull-Clark parametrisation remained equivalent.

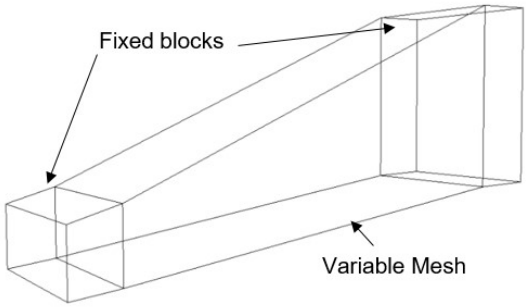

Figure 4.2: BlockMesh configuration integrating fixed and variable meshes.

The mesh stitching process required both the fixed Pointwise model and the variable blockMesh model to be in the same directory. The OpenFoam command "mergeMeshes Pointwise blockMesh –overwrite" was executed to consolidate the Pointwise mesh into the blockMesh diffuser model. The coordinates of the geometries had to be carefully assigned to ensure that the merging inlet and outlet were aligned. Within the 0 directory appropriate boundary conditions for all patches, including the adjoining patches, for each physical fluid flow quantity were specified. The adjacent patches were interconnected using the "stitchMesh masterOutlet slaveInlet –overwrite" operation. This caused the previous boundaries masterOutlet and SlaveInlet to have no cells assigned to them, effectively eliminating their existence. Flow could then be simulated through the entire mesh from prescribed inlet velocity and outlet pressure.

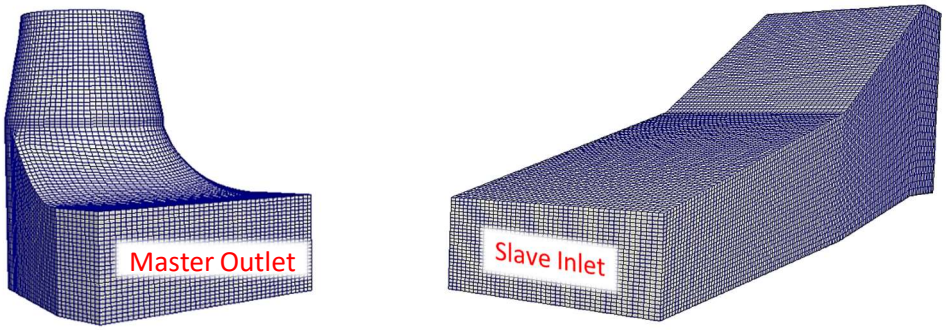

Figure 4.3.: Mesh resolution of stitched patches.

The cell size of the constant Pointwise mesh was determined by an appropriate first node wall distance at the inlet to achieve a non-dimensional wall distance (y^+) of 30. This cell size evolved through the elbow of the geometry to the rectangular cross-section of the integrated patch. The resulting hexahedral cell structure had 27 cell division in the y component and 44 cell divisions

in the Z component. The corresponding y^+ value at the integrated patch, calculated from the mean velocity at the cross-section was 18.42. The minimum required y^+ value quoted for the k-epsilon turbulence model is 30. The disparity of y^+ emphasises the challenge in producing a high quality mesh that converges towards the true draft tube geometry while also needing to satisfy a relatively large minimum cell height at the boundary. The challenge is exacerbated by the decelerating flow through the draft tube geometry further increasing the minimum cell wall size as the cross sections increase. In order for the group project to progress, the required y^+ values were compromised. Hardy's individual report investigated the use of different turbulence models with more appeasing y^+ requirements eradicating the low y^+ issue.

Table 6: Cell construction of outlet diffuser.

Y Dimensions of Stitch Patched (m)	Z Dimensions of Stitch Patched (m)	Cell Number in the Y Dimension	Cell Number in the Z Dimension	First Node Wall Distance (m)	Resultant y^+
0.01983	0.05	27	44	0.000734444	18.42

In an effort to pre-empt problematic poor mesh quality between the integrated patches previously experienced in the literature, the cell structure of the constant Pointwise outlet was replicated by the blockMesh inlet [28]. Figure 4.3 shows the integrated patch cell structure of the Pointwise outlet that blockMesh is capable of replicating. BlockMesh demands a ridged, structured topology, where the number of faces between interconnecting blocks are conserved. Therefore, the cross-sections of the outlet diffuser mesh will always comprise of a grid formation with 27 rows along the y component and 44 columns along the z component.

4.3. Automation of BlockMeshStitch Model

Python scripting was used to automatically mesh and simulate the optimiser requested geometry. Spline coordinates requested for evaluation were imported to the constant/polymesh directory of the variable blockMesh model. A python script was then executed to generate the blockMesh dictionary where the spline coordinates were inserted as the interconnected points defined the B spline edges. This list of interpolation points is all that is required to establish a replica spline in the blockMesh dictionary to that of the optimised spline. The requested draft

tube geometry was then meshed using the sub processes command within python to execute the OpenFOAM mesh generating procedure. The simulation was run using the simpleFOAM steady state solver. Once the predefined number of iterations were completed, the pressure difference between the inlet and outlet was obtained by averaging the pressure patch faces. The calcPressureDifference command developed in work of Daniel and Rabat was directly apply to achieve this [20]. The optimisation code could then translate the pressure difference in terms of the objective function. Through the Bayesian optimisation technique the region of greatest expected improvement was determined, identifying where to sample next. The computational draft tube model is initialised after each simulation is complete by copying across from a base model file. The use of the CFD model by the optimisation is shown in the flow chart below.

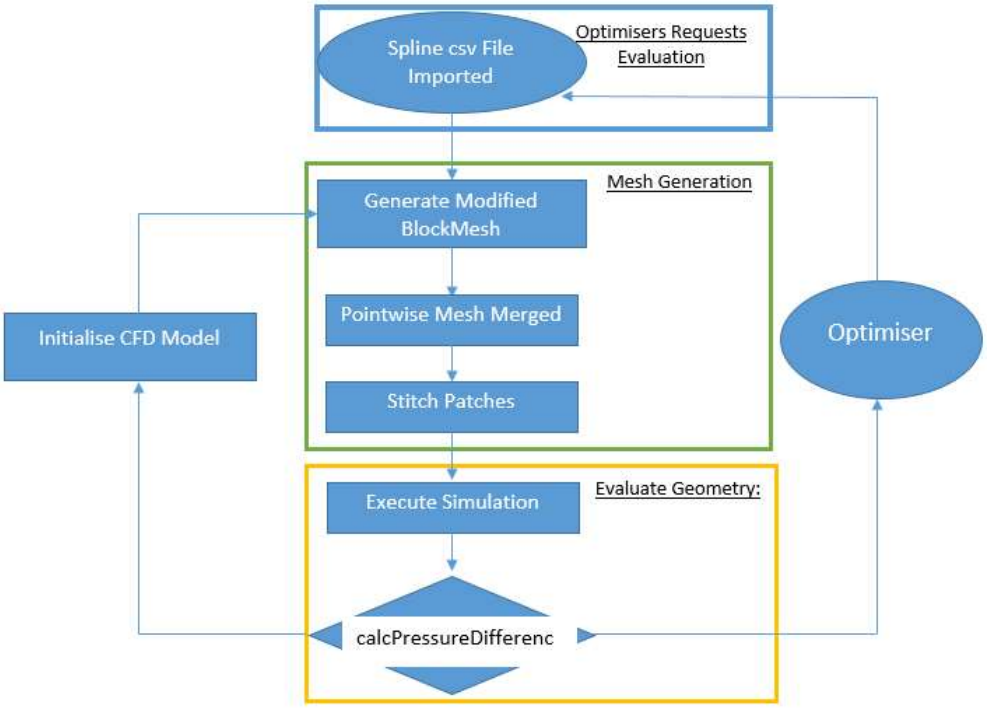

Figure 4.4: Flow chart visually representing automotive model.

4.4. Determining Feasible Bounding Box

The optimisation search space was limited to a region of potential designs through a coordinated defined bounding box. An initial bounding box based on the manufacturing constraints of the 3d printing process was provided. A previous study using the integration of fixed and variable meshes highlighted the importance of appropriate potential design constraints that accommodated the meshing technique [28].The blockMesh generator struggled to apply the rigid, structured, hexahedral mesh elements to extreme curvature. The performance of the BlockMeshStitch model was investigated for splines extending to outer limits of the

boundary box. The meshing method was unable to generate meshes capable of stable simulations for geometries at the outermost of the experimental bounding box.

The performance of the model was systematically evaluated for a reduced bounding box. The control points governing the spline locations were moved across small intervals to reduce curvature. The resulting bounding box illustrated in figure 4.5, represents the outermost location of the experimental bounding box where stable simulations were achieved. Fixed control points close to the location of reattachment to the fixed geometry, were also introduced to further mitigate against excessive curvature. The establishment of suitable design constraints allowed additional geometries to be requested for experimental analysis.

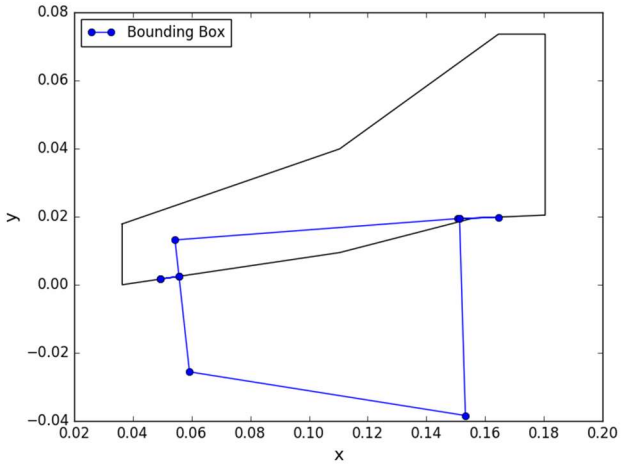

Figure 4.5: Feasible bounding box for the BlockMeshStitch model.

4.5. Analytic Result of BlockMeshStitch Model

The predicted pressure recovery factor against the experimental results are shown in figure 4.6. The purpose of the computational model is to provide evaluative data to enable a near optimum relationship between draft tube geometry and pressure recovery to be established. The modelled results demonstrate reasonable agreement with the experimental results. Importantly, the simulated results display the same trends of model performance as the experimental results. However, the computational results repeatedly overestimate the pressure recovery and are unable to fully distinguish the change in performance between the top and bottom spline altered geometry. This indicates that the model may struggle to fully exploit the design space as modelling error could influence the optimised result. However, the ability to capture trends would enable the identification towards a global maxima.

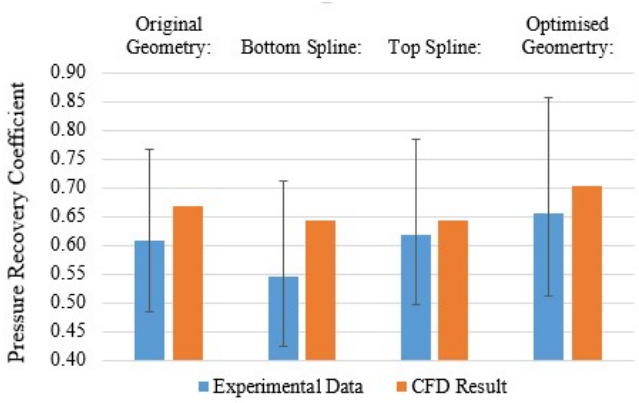

Figure 4.6: CFD predict pressure recovery factor against the pressure recorded from experimentation.

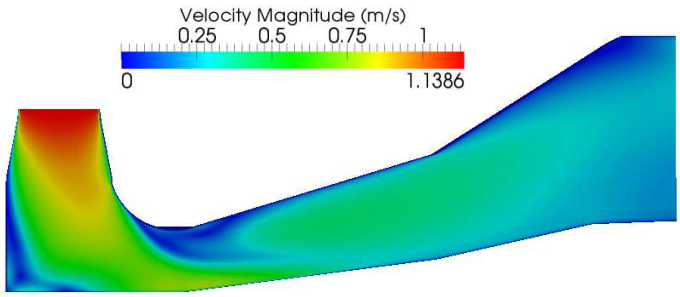

Figure 4.7: Velocity distribution of the original draft tube model.

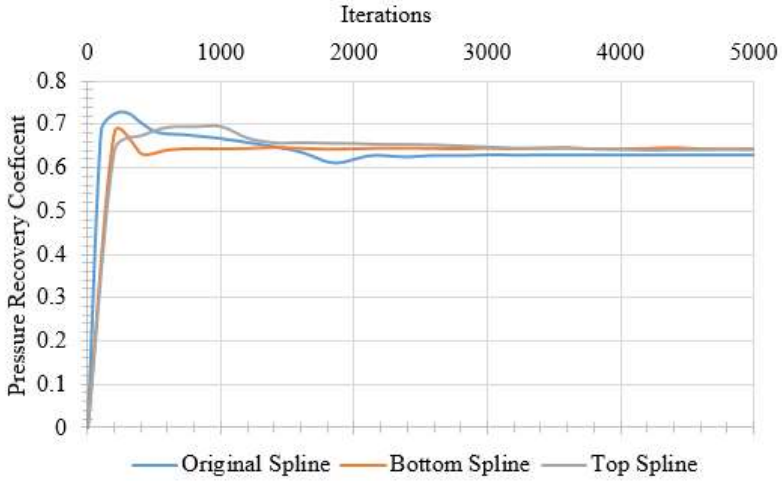

Figure 4.8: Variation in predicted pressure recovery with iterations.

The pressure recovery coefficient produced by the model was constant after 2000 iterations. Therefore, there is no advantage to be gained from an optimisation perspective to continue the simulations after 2000 iterations. The pressure recovery factor for the alter top and bottom spline geometries is stable after 1500 iterations. This could justify the reduction of iterations in order to reduce the computational intensity of the model.

The error residuals fail to fall below 0.001 as iterations increased. The experimental results concluded that the draft tube flow had transient properties [26]. The steady state simulation of a transient flow problem is responsible for the failure of residuals to converge. These error residuals were expected form the previously published literature, where it was concluded optimisation is still achievable without the convergence of error residuals [7].

4.6. Control Point Sensitivity Study

Monte Carlo sensitivity analysis was carried out on the BlockMeshStitch study to analyse its response to geometry potentially requested for optimisation. A Latin hypercube sampling strategy was used. 10 randomly generated splines geometries for 1 to 10 control points were simulated. The results illustrate the models in ability to evaluate irregular geometries generally produced by an increased number of control points. Failure of simulations occurred from all samples containing 4 or more control points. This failure of simulations suggests the inability of a structured meshing strategy to be synchronised with automatic optimisation likely to demand abnormal geometries.

Table 7: Failed simulations of the ten attempted.

Control Points	Number of Failed Simulations
1	0
2	0
3	0
4	2
5	3
6	4
7	1
8	4
9	7
10	6

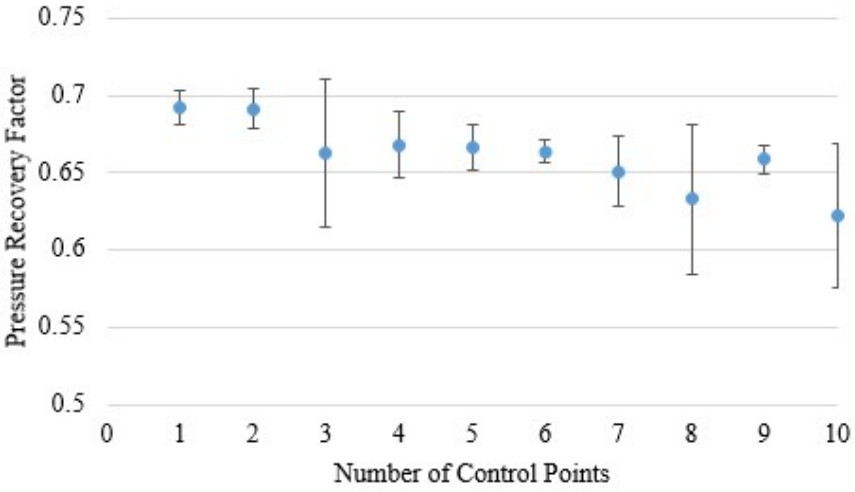

Figure 4.9: Average pressure recovery and standard deviation of sensitivity analysis.

The low standard devations indicate the lack of infulence the outlet diffuser has on the pressure recovery factor of the draft tube. This increases the emphasis on the accuracy of the model required to exploit minor improvements.

5. Inlet Conditions

The need for an in-depth understanding of inlet conditions motivates a large proportion of the literature surrounding the computational modelling of draft tubes [5]. However, the experimental team were unable to replicate swirling inlet flow with the limited equipment

available [26]. For effective validation of computational results, it is essential that the flow case model matches the experimental case. Therefore, the complex flow characteristics that have posed major challenges in previously published work were simplified in order to match the experimental case.

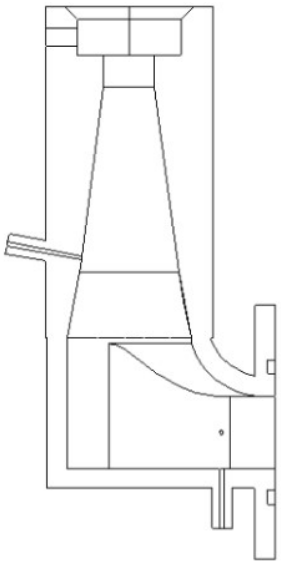

Figure 5.1: CAD drawing of pre inlet experimental set up.

The pre-draft tube experimental set up is shown in figure 5.1. The pipe network connecting the draft tube inlet to the flow bench exhibits a cone diffuser followed by a sudden contraction in the pipe's cross section. Therefore, the turbulent flow at the inlet was expected to have regions of separation and other complex flow characteristics. The development of correct inlet conditions is a vital deliverable to the group project. The optimisation process requires the accurate simulation of draft tube flow, which is dependent on representative inlet conditions.

5.1. Inlet Velocity Profile Sensitivity Study

A preliminary study investigated the sensitivity of the pressure recovery factor to a range of empirical velocity profiles. The empirical velocity profiles applied at the inlet were calculated with the assumption of fully developed flow along a uniform pipe. The equation defined velocity profiles were implemented onto the BlockMeshStitch draft tube model through OpenFOAM add-on Swiss Army Knife for OpenFOAM (SWAK4FOAM), which caters for a greater variety of inlet flow conditions. The applied empirical velocity profiles are shown in figure 5.2.

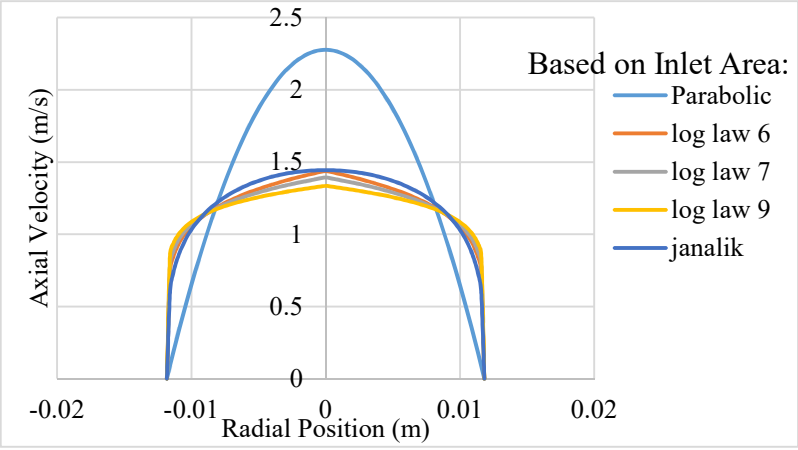

Figure 5.2: Empirical velocity profiles applied to the inlet of the numerical draft tube model.

Parabolic Velocity Profile:

A parabolic velocity profile is normally considered for laminar flow, where viscous forces dominate as the effects of the no slip conditions at the wall are significant. This inlet condition is often considered for turbulence modelling of confined geometry where the boundary layer overlaps.

$$v = 2.v_{(av)}\left[1 - \left(\frac{r}{R}\right)^2\right]$$

Equation 8: Parabolic Velocity Profile. **[31]**

v = Velocity (m/s)
$v_{(av)}$ = Average Velocity (m/s)
r = radial position (m)
R= Outer Pipe radius

Power Law Velocity Profile:

Increased turbulent flow is estimated with a power law velocity profile. From calculations a log law 6 velocity profile would be most appropriate to this case. The maximum velocity was obtained by the integration of the power law velocity profile.

$$v = \frac{v_{(av)}}{2}.\left(\frac{1}{n}+1\right).\left(\frac{1}{n}+2\right)\left[1 - \frac{r}{R}\right]^{1/n}$$

n = Turbulence coefficient

Equation 9: Expanded Power Law Velocity Profile **[31]***).*

Turbulent velocity profile Munson, 2008:

The Munson velocity profile is a more recently developed velocity profile for turbulent pipe flow that demonstrates a smoother curve to the centre of the pipe.

$$v = v_{(av)}.(n_0+1).\left[1 - \left(\frac{r}{R}\right)^2\right]^{n_0}$$

Equation 10: Munson Velocity Profile **[32]**.

$$\frac{1}{n_0} = 1 + \sqrt[6]{\frac{Re}{50}}$$

Equation 11: Munson Velocity Profile Coefficent **[32]**.

These empirical velocity profiles were applied to the original draft tube case as well as the request top and bottom spline geometries documented in Angus's individual report [26]. The simulated results were compared with experimental data.

5.2. Development of CFD Estimated Inlet Profile

The irregular geometry of the experimental set up before the draft tube inlet violated the assumptions of fully developed uniform pipe flow that is required for the application of empirical velocity profiles. Due to the small scale of the experimental set up, it was not possible to gain experimental data regarding the velocity profile at the inlet. Therefore, a CFD solution to determine the experimental inlet velocity profile was proposed.

The pre-inlet experimental set up was simplified as a straight thin pipe followed by a sudden extension and then a cone diffuser. The dimensions of the model matched the computer aided drawing defined for the 3d printing manufacturing process of the experimental draft tube. At the time of modelling, the length of the thin pipe was not established. Therefore, a pipe length over the entrance length of the flow conditions was used.

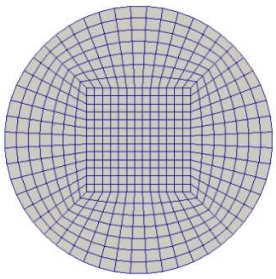

Figure5.4: O-H grid topology at cone outlet.

Figure 5.3: Estimated pre-inlet geometry

The meshing strategy used to discretise the pre-inlet model's geometry was the stitching of structures meshes generated in blockMesh, building on the techniques learnt through the development of the BlockMeshStitch model. An O-H topology mesh was used to minimise the skewness of cells from fitting the hexahedral elements to the circular geometry. The thin pipe geometry was stitched to the pipe expansion and cone. A multi block mesh with a consistent core of a square cross section encapsulated by four arced blocks was generated for the thin pipe. The sudden expansion pipe and cone diffuser consisted of an identical mesh core to allow for a smooth mesh stitching process. Four additional curved blocks were joined to the outside of the mesh core to achieve the desired expansion.

A high quality mesh was established through experimentation in the mesh density and size of the square core within the O-H grid. The literature is vague on the best ratio between the square core and external curved blocks with modeller's intuition being stated as the best approach to find a suitable ratio [25]. The mesh density was increased proportionately along the radial axis with the objective to determine a mesh independent solution. For every case in the mesh refinement study, the first wall distance satisfied the K-epsilon turbulence modelling range criteria of 2 to 150 with an approximate average of 30. The high velocity flow within a uniform geometry made y^+ values of 30 achievable. A uniform inlet velocity of $8.811 ms^{-1}$ was defined in coherence with the targeted experimental flow rate. The boundary conditions applied to the outlet of the pre-inlet model was a relative pressure of 0 Pa. Once an appropriate inlet velocity profile was established, a replica function was determined using a regression analysis tool available in Microsoft Excel. The estimated profile was then applied through SWAK4FOAM.

Table 8: Characteristic of flow at the different sections of the pre-inlet model.

	Thin Pipe:	Fat Pipe:	Cone:
Diameter (m)	0.0085	0.0127	0.023646
Average Velocity (m/s)	8.811	3.947	1.139
Reynolds Number:	57304	38353	20599

5.3. Results of Inlet Velocity Profile Sensitivity Study

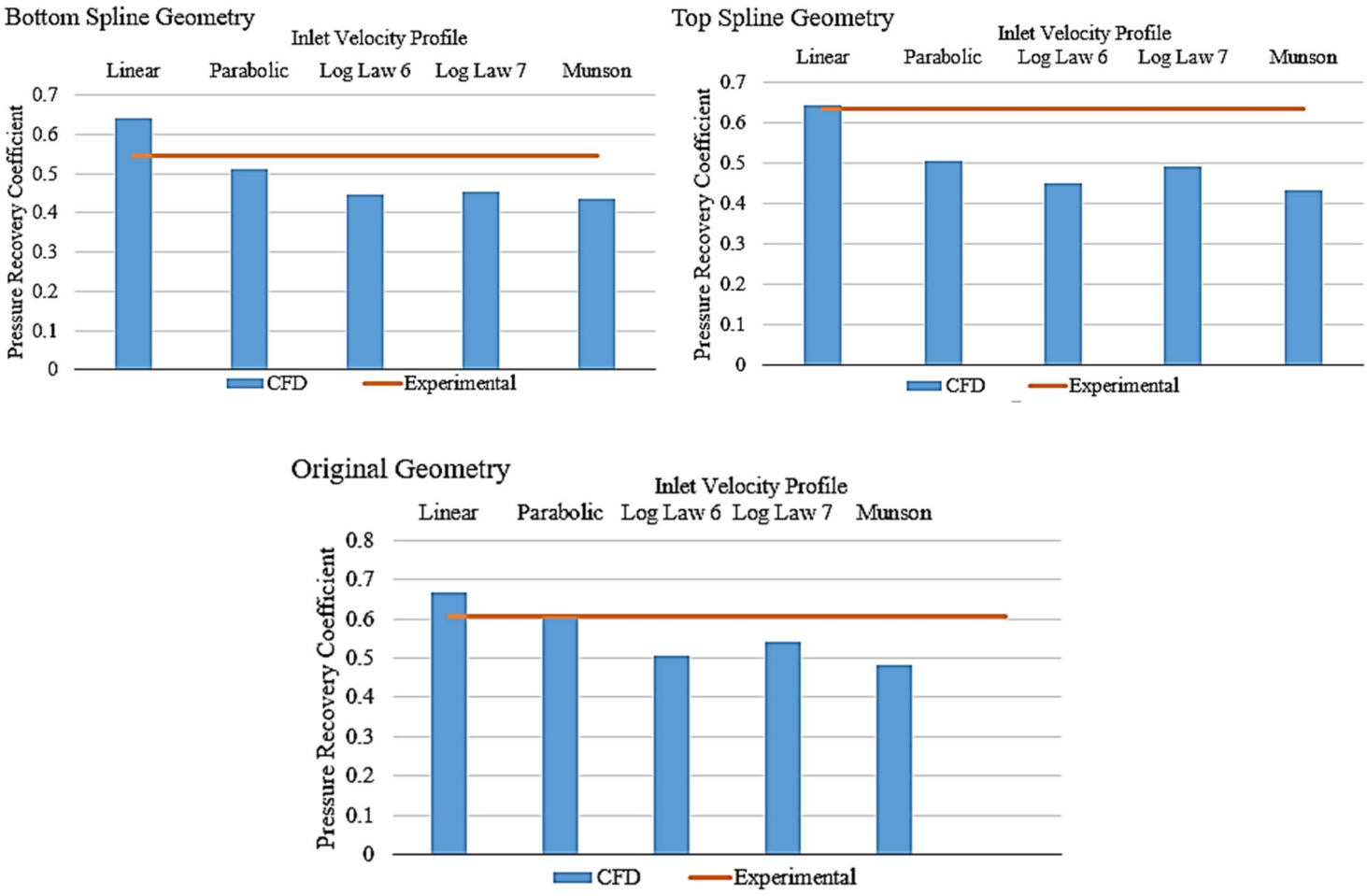

Figure 5.5: Sensitivity of modelled results to the define inlet velocity across three draft tube geometries.

The results show substantial sensitivity to the applied inlet velocity profile with a flat linear profile producing a higher pressure recovery factor than the empirical formulas. The prescribed

velocity that provides the closest simulated solution to the experimental data varies between the flat velocity profile and the parabolic profile. The inaccuracy of the empirical formulas confirm the undeveloped nature of the turbulent flow at the inlet. The inlet velocity profile has little influence on the computational models ability to identify the most efficient draft tube. Across the three geometries the original design consistently produced the highest pressure recovery. This is significant with regards to the overall project objective as high preforming draft tubes can still be identified by the numerical models with constant velocity applied at the inlet. In this case the velocity profile appears to act more as an offset than a significant feature that would influence the optimisation.

5.4. Results of CFD Estimated Inlet Profile

The proportion of the square in the O-H grid topology had no effect on the outlet velocity profile. The mesh with a structure ratio of 0.55 produce the lowest non orthogonal statistics and was used for the mesh density study. The results from the mesh density study show the solutions begin to diverge at an element size of 0.24 mm^3 as the refinement level induces a catastrophic mesh quality. However, the relatively small change in velocity profiles, despite a cell count increase of over 100,000 elements, indicates the solution is mesh independent.

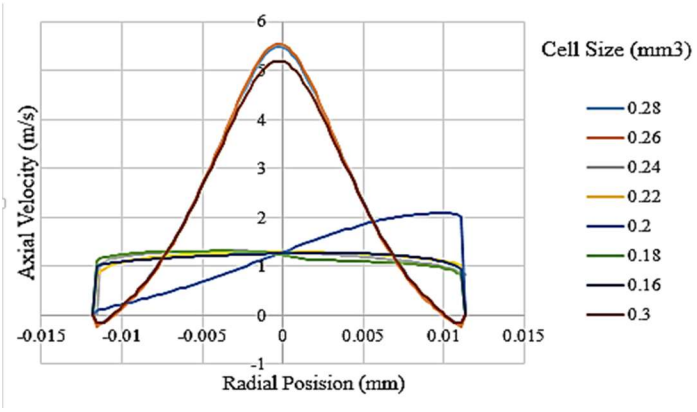

Figure 5.6: Effect of the mesh density to outlet velocity profile.

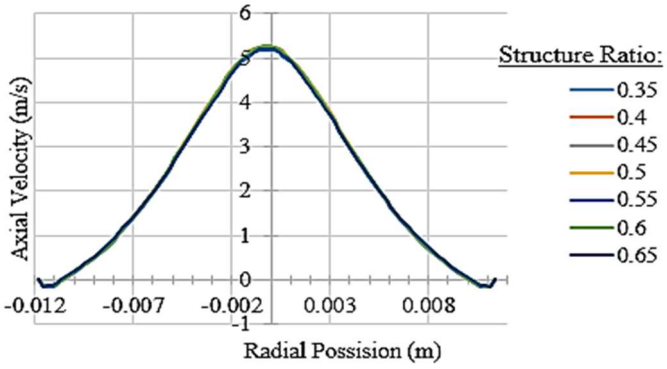

Figure 5.7: Effect of structure ratio to outlet velocity profile.

The pre-inlet computational model predicts a narrowed velocity profile with a high peak velocity when compared to the empirical profiles. The recirculation region caused by the sudden pipe expansion is still present in the velocity profile at the draft tube inlet with a small negative velocity close to the wall at the outlet. The separation region reduced the effective cross-section in the cone diffuser, thus increasing the freestream velocity and resulting in a narrowed velocity profile.

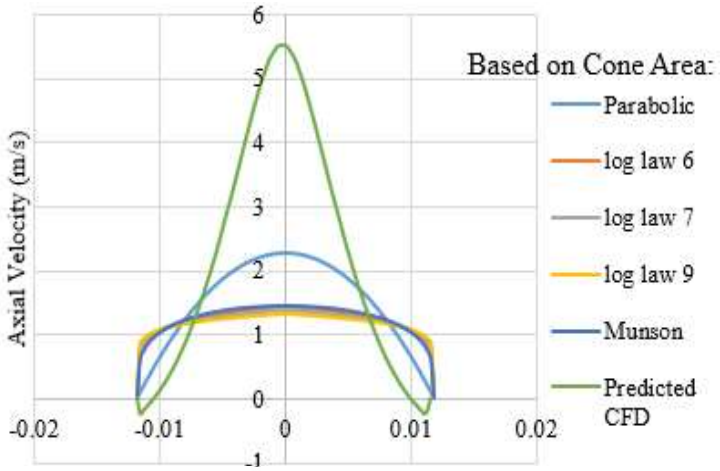

Figure 5.8: Predicted outlet velocity profile compare to empirical formulas.

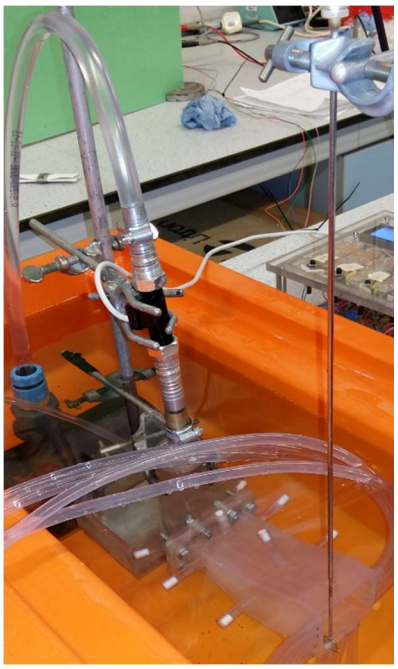

Figure 5.9: Experimental Set

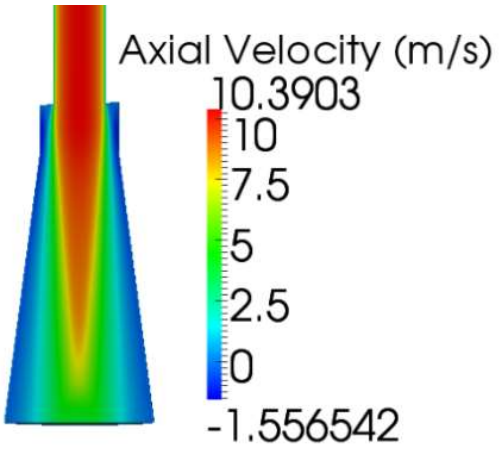

Figure 5.10: Velocity distribution at the cone diffuser.

The draft tube simulations with the CFD estimated velocity profile superimposed, produced a pressure recovery twice as large as the experimental result. The over simplification of the pre inlet CFD model is the most likely cause of this significant error. The true pre inlet set up is shown in figure 5.9. The computational model did not incorporate the curvature of the pipe feeding the cone diffuser or disruption caused by the flow sensor equipment.

Table 9: Simulated pressure recovery of draft tube models with predict inlet velocity profile super imposed.

	Original Geometry	Bottom Spline	Top Spline
Experimental Pressure Recovery Factor	0.60634322	0.54448942	0.631658976
Simulation Pressure Recovery Factor	1.271499263	1.173632257	1.19956547

6. Discussion and conclusions

6.1. Discussion

The use of the rigid, structured meshing strategy employed by the BlockMeshStitch produced high mesh quality for uniform shapes, but struggled to produce meshes capable of stable simulations for irregular geometries. It was able to determine trends between draft tube geometries and the pressure recovery factor. This enabled the use of the model for optimisation purposes. However, table 10 shows the accuracy of BlockMeshStitch modelled results is lower when compared to the Pointwise and cfMesh automatic models developed within the group project. [3] The accuracy of simulations is of great importance due to the reduced sensitivity of pressure recovery to geometric change when only optimising the diffuser of the draft tube. The disparity between the more accurate structured Pointwise and the structured BlockMeshStitch results shows that modelling error is induced by the stitching of fixed and variable meshes.

The block mesh stitch model was synchronised to the optimisation code and was able to predict an improved design for 1 and 2 control points. However, the inability of the BlockMeshStitch model to mesh irregular geometries limited the number of optimisation variables to two control points. Unstructured meshing approaches proved to be sufficiently robust, able to model a higher number of control points. The potential for abstract designs due to the Catmull-Clark parametrisation clashed with the BlockMeshStitch models lack of flexibility around the fixed meshes.

The mesh generation and run time of the BlockMeshStitch was 1,200s on a computer with 4 cores and 16 gigabytes of ram. The optimiser required $(11 \times no.of\ dimensions) - 1$ simulations for the initial samples and then a further 100 simulations. The optimisation process took 36 hours for one control point and 40 hours for two control points. This means the optimiser could be run over the weekend in an industry environment utilising out of office hours.

Table 10: Variation of modelling techniques developed within the group project.

	Experimental Maximum	Experimental Minimum	Experimental Mean	BlockMeshStitch	Pointwise	cfMesh
Original C_p	0.646	0.570	0.608	0.665	0.617	0.612
Bottom Spline C_p	0.599	0.493	0.546	0.642	0.448	0.563

The BlockMeshStitch model was able to be used in the prediction of a near optimal shape. However, for this problem case accuracy of the solutions was of paramount importance and the parameterisation demanded high robustness. Therefore, other methods developed with the group project would be more suitable. The model was effectively used for sensitivity analysis, as its desirable run time allowed for large levels of data to be amassed.

The simulated results were proven to be sensitive to the applied inlet velocity profile. However, the relationship between the performance of the draft tube and changes in the geometry appeared to be conserved within reasonable assumptions for the velocity profile. Determining the inlet velocity profile of the draft tube through the superposition of a numerically predicted profile was unsuccessful. A more detailed pre-inlet computational model is required to accurately represent the inlet velocity profile of the draft tube. A better approach would be to directly apply recorded experimental results to the CFD model, however this was not possible due to the experimental set up.

6.2. Conclusion

An automatic model that combined a fixed Pointwise mesh and a variable blockMesh provided function evaluations for the optimisation of a draft tube. The reduction in mesh size required to be generated for each evaluation ensured a computationally efficient model. The use of structured meshing techniques limited the number of variables for the optimiser compared to more robust unstructured meshing strategies. Therefore, the use of blockMesh could only achieve optimisation of a draft tube parameterised with two control points. Comparisons between the BlockMeshStitch model and the Pointwise model indicates the stitching of meshes increases modelling error.

The sensitivity of the draft tube model simulations to prescribe inlet velocity profiles was significate. However, the performance of the draft tube and changes in the geometry appeared to be conserved within reasonable assumptions for the velocity profile. Therefore, the project's use of a linear inlet velocity profile for the optimisation of the draft tube was acceptable.

6.3. Future Work

The group project as a whole recognised that the parametrisation of the draft tube should expand beyond the outlet diffuser and explore more aspects of the draft tube geometry. Therefore, the parameterisation would include a combination of cross-sectional profiles. The

use of blockMesh to integrate across varying cross-sections of different shapes would need to be investigated. Especially the potential of using the O-H grid topology to evolve from a circle into a square profile. The increased parametrisation could reduce the susceptibility of requested geometries having localised extreme curvature, which proved problematic for structured meshing techniques.

The establishment of representative inlet flow conditions is a key component for future work. The failure to determine inlet conditions from a simplified computational model of pre inlet condition emphasises the need for experimental data to be directly applied to the numerical draft tube model.

7. Project management

7.1. Management Practices

Weekly group meetings provided the opportunity to update fellow group members and the project supervisor on the progress made towards the project aim. These meeting steered the direction of the project allowing group feedback on individual work packages and operated as a corrective mechanism to reduce deviation from the critical path of the project. A meeting chair and secretary was assign to each weekly meeting. The predetermined agenda would be discussed and meeting minutes were recorded. A google drive was employed for formal documentation of critical documents.

A project forum was set up on Facebook, as it was deemed the most accessible and regularly checked communication tool by group members. This allowed for constant communication between group members and automatically logged information shared. The CFD sub team identified the importance of a communal work space to increase productivity and ensure individual developments in the understanding of OpenFOAM could be shared. Configuration management of computational models was implemented through the use of a shared external hard drive. Baseline models representing major developments in the project were archived by the hard drive. A spread sheet on the hard drive detailed the differences between models.

7.2. Establishment for Critical Deliverables

The key deliverables on the critical path of the project were identified. The philosophy of the project was to focus on establishing the simplest possible case, which could then be improved upon. Mitigation actions were taken in the event of delays to mandatory tasks key to achieving the group objective. There were delays in recording experimental results. Members of the CFD and optimisation sub teams help in the manufacturing of the experimental set up. Further delays in obtaining experimental results led to the optimisation process being executed before model validation took place.

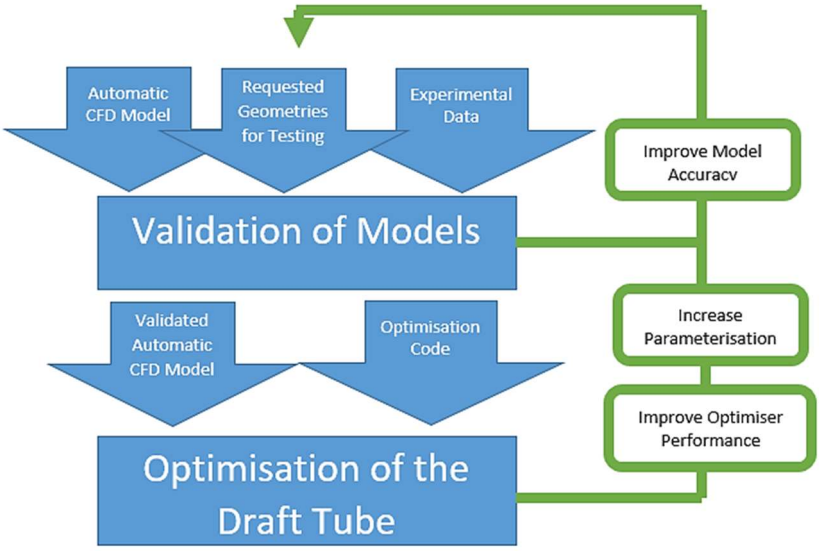

Figure 7.1: Flow chart of key deliverables in the project.

8. Contribution to group functioning

The work documented in this individual report contributed to the optimisation of a draft tube. The bounding box constraining the potential design space determined within this report ensured geometries requested for experimental data were within the simulating capabilities of the computational models.

The conclusions drawn from the investigation of inlet velocity profiles provided confidence in the validity of the optimisation process and was a key contributor ensuring group deliverable IV was achieved [3].

The BlockMeshStitch model was compatible with the optimiser code developed by the optimisation sub team. The modelling approaches diversified the results of the group allowing for greater comparison between models developed within the CFD sub team.

9. References

[1] B. D. Marjavaara, “Turbine Diffuser Shape Optimization by Multiple Surrogate Model Approximations of Pareto Fronts,” *Journal of Fluids Engineering,* vol. 129, no. 9, pp. 12 - 28, 2007.

[2] S. Galván, “Numerical optimization of the inlet velocity profile ingested by the Conical draft tube of a hydraulic turbine,” *Journal of Fluids Engineering,* vol. 137,no. 7, p. 071102, March 2015.

[3] P. Burns, S. Hardy, R. Gilbert, J. Angus, T. Dye, C. Ng, S. Hutchings and J. Gowans, “G2 Report: An investigation into the Optimisation of a Draft Tube,” Univerisity of Exeter, Exeter, 2017.

[4] J. McNabb, “CFD based draft tube hydraulic design optimization,” in *IOP Conference Series: Earth and Environmental Science*, 2014.

[5] S. Galvan, F. Guibault and M. Reggio, “Optimization of the inlet velocity profile of Turbine-99,” in *Proceedings of the third IAHR/ERCOFTAC workshop on draft tube flows, Turbine-99 III*, Porjus, 2005.

[6] U. Andersson, “Turbine 99 - Experiments on draft tube flow (test case T).,” Orebro, 2000.

[7] H. NILSSON, “Evaluation of OpenFOAM for CFD of turbulent flow in water turbines,” Goteborg, Sweden, 2006.

[8] H. Ying, “Computer simulation of turbulent flow through a hydraulic turbine draft tube,” *Wuhan University, Journal of Natural Sciences,* vol. 11, no. 3, pp. 649-652, 2006.

[9] T. C. Vu, “Steady and unsteady flow computation in an elbow draft tube with experimental validation,” vol. 4, no. 1, pp. 85-96, 2011.

[10] M. Cervantes and U. Andersson, “Turbine-99 unsteady simulations – Validation,” *IOP Conference Series: Earth and Environmental Science,* vol. 12, no. 210, pp. 1 -10, 2005.

[11] A. E. Lyutov, “Coupled Multipoint Shape Optimization of Runner and Draft Tube of Hydraulic Turbines,” *Journal of Fluids Engineering,* vol. 137, no. 11, 2015.

[12] B. Marjavaara, “Parameterisation and flow design optimisation of hydraulic turbine draft tubes,” vol. 32, no. 5, 2004.

[13] E. P. R. Institute, Hydro Life Extension Modernization Guides: Volume 2: Hydromechanical, EPRI, 2000.

[14] T. C. Vu, “Viscous flow analysis as a design tool for hydraulic turbine component” *Journal of Fluids Engineering* vol. 112, no. 1, 1990. No journal

[15] R. Khare, “Numerical study on performance characteristics of draft tube of mixed flow hydraulic turbine," Hydro Nepal: *Journal of Water Energy and Environment,* vol. 10, no. 1, 2012.

[16] R. EISINGER, “Automatic Shape Optimisation of Hydro Turbine Components Based on CFD,” Stuttgart, Germany, 2001.

[17] J. A. Samareh, “Geometry and Grid/Mesh Generation Issues for CFD and CSM Shape Optimization,” *Optimization and Engineering,* vol. 6, no. 1, pp. 21 - 32, 2005.

[18] J. Hellström, “Parallel CFD simulations of an original and redesigned hydraulic turbine draft tube,” *Advances in Engineering Software,* vol. 38, no. 5, pp. 338-344, 2007.

[19] S. Hutchings, *Surface Representation and Parameterisation for Optimisation,* Exeter, 2017.

[20] S. Daniels and et. al, *A review of shape distortion methods available in the OpenFOAM framework for automated design optimisation,* Exeter: NA, 2017.

[21] OpenCFD, “OpenFOAM User Guide,” OpenCFD Ltd (ESI Group), [Online]. Available: http://www.openfoam.com/documentation/user-guide/. [Accessed 3 5 2017].

[22] B Fabritius, G Tabor, “Improving the quality of finite volume meshes through genetic optimisation,” *Engineering with Computers,* vol. 32, no. 3, pp. 425-440, 2015.

[23] S. Hardy, *Automatic Mesh Generation for Shape Optimisation of a Draft Tube Using cfMesh,* Exeter, 2017.

[24] J. Rhoads, “Effects of grid quality on solution accuracy,” 2014.

[25] A. Meister, Hyperbolic Partial Differential Equations, Wiesbaden: Vieweg+Teubner Verlag, 2002.

[26] J. Angus, *Experimental Investigation of Flow Inside Draft Tubes with Varied Diffuser Geometry,* Exeter, 2017.

[27] J. Gowans, *Automatic structured and unstructured mesh generation using Pointwise,* Exeter, 2016.

[28] J. Janusevskis and R. L. Riche, “Robust optimization of a 2D air conditioning duct using,” *hal.archives-ouvertes,* vol. 3, no. 12, pp. 1-12, 2011.

[29] D. Marjavaara, CFD driven optimization of hydraulic turbine draft tubes using surrogate models, Luleå: Division of Fluid Mechanics, Luleå University of Technology, 2006.

[30] Fureby, H.G Weller G Tabor H Jasak C, “A tensorialrial approach to computational continuum mechanics using object orientated techniques,” vol. 12, no. 6, p. 620 to 631, 1998.

[31] S. Pope, Turbulent Flows, Cambridge University Press, 2008.

[32] B. Munson, Fundamentals of Fluid Meshanics, John Wiley and Son, Inc, 2006.